13. The expected amplitude of the average of N trials with randomly distributed phase is $1/\sqrt{N}$ of mean single-trial amplitude. On average, the single-subject ERPs were averages of 922 trials, so the expected mean |ERP|/|EEG| amplitude ratio was $1/\sqrt{922}$ = –29.65 dB.
14. S. Makeig, *Electroencephalogr. Clin. Neurophysiol.* **86**, 283 (1993).
15. Time/frequency analyses used three-cycle Hanning-windowed sinusoidal wavelets at each frequency moved through the 3-s data epochs (from –1 s before to 2 s after stimulus onset) in 14-ms steps. Event-related spectral perturbation (ERSP) plots showed time/frequency points at which mean log power, across the input epochs, was higher or lower than mean power during the 1-s prestimulus baseline period of the same epochs. The ERSP transform of the averaged ERP data (Fig. 1C) was computed for each scalp channel across the 15 individual-subject ERPs. The ERSP transform of the single-trial epochs (Web. fig. 3B) was computed, for each subject and scalp channel, across a mean of 922 single-trial epochs. Bootstrap $P < 0.02$ significance levels were computed from distributions of ERSP values computed from surrogate data windows drawn at random from the same data epochs.
16. Also referred to as "phase-locking factor." [C. Tallon-Baudry, O. Bertrand, C. Delpuech, J. Pernier, *J. Neurosci.* **16**, 4240 (1996)]. Window lengths, step size, and significance levels were the same as for the power analyses (*15*).
17. These results parallel the demonstration of Sayers *et al.* (*2*) that the averaged auditory ERP in their experiments was produced by a stimulus-induced partial phase resetting of EEG rhythms in single trials.
18. These data used a right mastoid reference. Similar relationships between alpha phase and subsequent ERP morphology have been reported by B. H. Jansen, M. E. Brandt, *Electroencephalogr. Clin. Neurophysiol.* **80**, 241 (1991), and related results in (*19–21*).
19. M. E. Brandt, *Int. J. Psychophysiol.* **26**, 285 (1997).
20. R. Barry, S. Kirkaikul, D. Hodder, *Int. J. Psychophysiol.* **39**, 39 (2000).
21. V. Kolev, J. Yordanova, M. Schurmann, E. Basar, *Int. J. Psychophysiol.* **39**, 159 (2001).
22. S. Makeig, A. J. Bell, T.-P. Jung, T. J. Sejnowski, *Adv. Neural Inf. Process. Syst.* **8**, 145 (1996).
23. T.-P. Jung *et al.*, *Proc. IEEE* **87**, 1107 (2001).
24. A. J. Bell, in *Handbook of Neural Networks*, M. Arbib, Ed., in press.
25. A. J. Bell, T. J. Sejnowski, *Neural Comput.* **7**, 1129 (1995).
26. For each subject, ICA training data consisted of approximately 922 concatenated 52-point, 31-channel data epochs. Initial learning rate was 0.004; training was stopped when learning rate fell below 10^{-6}. Initial block size was 128. Training required less than 30 min per subject on a PC workstation. Source and binary code for the enhanced version (*24*) of the infomax ICA algorithm (*25*) we used are available, together with a MATLAB toolbox for EEG time/frequency analysis and visualization, from www.sccn.ucsd.edu.
27. A relatively large ICA training data set (31 channels by 150,000 time points) was used for maximum stability assuming similar early visual processing in all conditions. Detailed comparisons of different stimulus and attention conditions including target trials will be pursued in future studies.
28. Clustering was based on normalized component activity spectra and scalp maps, and used a modified Mahalanobis distance metric [S. Enghoff, "Moving ICA and time-frequency analysis in event-related EEG studies of selective attention," *INC-9902* (Institute for Neural Computation, La Jolla, CA, 1999)].
29. BESA software (Megis Software, Munich) [M. Scherg, D. v. Cramon, *Electroencephalogr. Clin. Neurophysiol.* **62**, 32 (1985)] was used to fit one or more dipoles to each ICA component scalp map using a four-shell spherical head model.
30. R. Hari, R. Salmelin, J. Makela, S. Salenius, M. Helle, *Int. J. Psychophysiol.* **26**, 51 (1997).
31. G. Pfurtscheller, C. Neuper, G. Krausz, *Clin. Neurophysiol.* **111**, 1873 (2000).
32. S. Makeig, S. Enghoff, T.-P. Jung, T. J. Sejnowski, *IEEE Trans. Rehab. Eng.* **8**, 208 (2000).
33. A. Rougeul-Buser, P. Buser, *Int. J. Psychophysiol.* **26**, 191 (1997).
34. A. Destexhe, T. J. Sejnowski, *Thalamocortical Assemblies* (Oxford Univ. Press, Oxford, 2001).
35. A. K. Engel, P. Fries, W. Singer, *Nature Rev. Neurosci.* **2**, 704 (2001).
36. R. Chapman, J. Stern, J. Engel, M. Cohen, "Tomographic Mapping of Alpha Rhythm Using Simultaneous EEG/fMRI," presented at the 7th Annual Meeting of the Organization for Human Brain Mapping, 10 to 14 June 2001, Brighton, UK (2001).
37. N. Logothetis, J. Pauls, M. Augath, T. Trinath, A. Oeltermann, *Nature* **412**, 150 (2001).
38. J. Klopp, K. Marinkovic, P. Chauvel, V. Nenov, E. Halgren, *Hum. Brain Mapp.* **11**, 286 (2000).
39. T. Mima, T. Oluwatimilehin, T. Hiraoka, M. Hallett, *J. Neurosci.* **21**, 3942 (2001).
40. A. Von Stein, C. Chiang, P. Koenig, *Proc. Natl. Acad. Sci. U.S.A.* **97**, 14748 (2000).
41. M. S. Worden, J. J. Foxe, N. Wang, G. V. Simpson, *J. Neurosci. Online* **20**, RC63 (2000).
42. G. D. Brown, S. Yamada, T. J. Sejnowski, *Trends Neurosci.* **24**, 54 (2001).
43. This research was supported by the Howard Hughes Institute for Medical Research, the NIH [NIMH 2RO1-MH36840 (E.C.) and NINDS 1RO1-NS34155 (J.T.)], the U.S. Office of Naval Research, the U.S. Fulbright Program, and the Swartz Foundation.

12 September 2001; accepted 12 December 2001

RNA Helicase MUT-14–Dependent Gene Silencing Triggered in *C. elegans* by Short Antisense RNAs

Marcel Tijsterman,* René F. Ketting,* Kristy L. Okihara, Titia Sijen, Ronald H. A. Plasterk†

Posttranscriptional gene silencing in *Caenorhabditis elegans* results from exposure to double-stranded RNA (dsRNA), a phenomenon designated as RNA interference (RNAi), or from co-suppression, in which transgenic DNA leads to silencing of both the transgene and the endogenous gene. Here we show that single-stranded RNA oligomers of antisense polarity can also be potent inducers of gene silencing. As is the case for co-suppression, antisense RNAs act independently of the RNAi genes *rde-1* and *rde-4* but require the mutator/RNAi gene *mut-7* and a putative DEAD box RNA helicase, *mut-14*. Our data favor the hypothesis that gene silencing is accomplished by RNA primer extension using the mRNA as template, leading to dsRNA that is subsequently degraded.

RNA interference (RNAi) in animals, co-suppression in plants, and quelling in fungi appear to be manifestations of cellular defense mechanisms against the invasion of foreign nucleic acids such as viruses or transposons. These gene-silencing phenomena share a common reaction intermediate: small RNA molecules [20 to 25 nucleotides (nt) long], designated siRNAs, that are complementary to the silenced locus and target the cognate mRNA for destruction (*1–5*). To study the role of such short RNA molecules in vivo and their dependence on genes required for RNAi (*6*, *7*), we examined whether we could trigger RNAi by injecting either single-stranded RNA (ssRNA) or double-stranded RNA (dsRNA) oligonucleotides into *Caenorhabditis elegans* (*8*).

Exposing *C. elegans* to *pos-1* dsRNA leads to embryonic lethality of the progeny (*6*). Because *pos-1* mRNA is maternally provided, one can administer the RNA oligomers into the immediate vicinity of the mRNA by injecting them into the gonadal syncytium. Injection of dsRNA molecules of 25 base pairs (bp), corresponding to the *pos-1* sequence (either blunt or with a 2-bp 3′ overhang), triggers gene silencing in 5 to 10% of the progeny embryos (Fig. 1). In contrast, injection of identical amounts of long dsRNA (0.8 kb) results in 100% RNAi, which is consistent with RNAi requiring long dsRNA to work efficiently (*5*). For the corresponding 25-oligomer ssRNAs, we found that although the sense oligomer had no effect, the antisense oligomer induced the RNAi phenotype in ~50% of the progeny when one gonad was injected and in 100% when both gonads were injected (Fig. 1A). The sequence context of the trigger did not strongly affect the efficiency of targeting; 25-nt antisense RNAs (asRNAs) complementary to different regions of the *pos-1* mRNA had similar abilities to induce gene silencing (Fig. 1B). The RNA nature of the trigger proved essential: Molecules

Hubrecht Laboratory, Center for Biomedical Genetics, Uppsalalaan 8, 3584 CT, Utrecht, Netherlands.

*These authors contributed equally to this work.
†To whom correspondence should be addressed at Hubrecht Laboratory, Uppsalalaan 8, 3584 CT, Utrecht, Netherlands. E-mail: plasterk@niob.knaw.nl

of identical sequence and base-pairing ability, such as DNA oligomers or morpholinos, were inactive (Fig. 1B), which argues against interference with the translation machinery. As was the case for RNAi triggered by long dsRNA molecules, 25-nt *pos-1* asRNAs produced "carriers": progeny animals that escape the immediate RNAi response but pass the phenotype on to their progeny. We conclude that short *pos-1* asRNAs are able to efficiently trigger gene silencing. This is in contrast to similar experiments that attempted to target the somatically expressed *unc-22* gene (*5*). We found that short *unc-22* asRNAs triggered RNAi in only 1% of the progeny, possibly because *unc-22* mRNA is not present in the injected tissue, and the ssRNAs are degraded before they can act in the soma.

To test this directly, we targeted green fluorescent protein (GFP) mRNA in animals that either expressed this reporter in the germ line or in somatic tissues. Injection of GFP asRNAs into *C. elegans* that have germline GFP results in a marked reduction of the GFP signal in the gonadal syncytium, the oocytes, and the developing embryos coming from the injected gonad (Fig. 1C). The loss of expression is confined to the injected gonad, indicating that, other than for long dsRNA, the asRNAs do not induce RNAi systemically. In contrast, we did not observe loss of GFP when GFP was expressed in a range of somatic tissues (*9*), which suggests that the time and range of target expression are crucial for the susceptibility of mRNA to asRNA triggers. A distinction between germline versus somatic expression is, however, not absolute; (i) we could trigger RNAi with *unc-22* asRNAs albeit with low frequency, and (ii) not all germline–expressed genes were susceptible (*9*).

Several RNAi-defective strains were assayed for their response to asRNAs: *rde-1* and *rde-4*, which are RNAi-deficient (*6*), and *mut-7* and *mut-14*, which are defective in RNAi as well as in transposition silencing and co-suppression (*7*, *10*). We found that RDE-1 and RDE-4 are not required for this type of gene silencing; in contrast, MUT-7 and MUT-14 proved essential: *pos-1* asRNAs failed to trigger gene silencing in *mut-7* and *mut-14* animals (Fig. 1D).

Are *rde-1* and *rde-4* animals incapable of producing siRNAs and do injected asRNAs functionally substitute for siRNAs, therefore bypassing the requirement for RDE-1 and RDE-4 in RNAi? To address this question, we assayed these mutants for their ability to produce siRNAs. RNase protection assays revealed that *pos-1* siRNAs are readily detectable in wild-type *C. elegans* undergoing RNAi (*11*) (Fig. 2A). In contrast, *pos-1* siRNAs are not detected in *rde-1*, *rde-4*, and *mut-7* mutant animals, which suggests that these proteins are involved in the first step in RNAi: processing of long dsRNA into siRNAs. However, cell-free extracts prepared from, for example, *rde-1* animals were fully proficient in dicing long dsRNA into siRNAs (*12*) (Fig. 2B). We therefore favor the explanation that *pos-1* siRNAs are produced in these animals but fail to form a stable complex allowing siRNA detection. In support of this idea, we found that although *C. elegans* extracts produced both sense and asRNA species, in vivo siRNAs had predominantly antisense polarity (Fig. 2D).

The observation that siRNAs are detected in *mut-14* animals suggests that MUT-14 is not essential for siRNA stabilization. *mut-14*(*pk738*) animals resemble *mut-7* animals in germ-line transposon activation, RNAi deficiency, resistance to co-suppression (*10*), transgene desilencing, high incidence of males, and sterility at 26°C. We cloned *mut-14* by genetic mapping and subsequent candidate gene approach (*13*) (Fig. 3). We found that *pk738* has a point mutation in the gene C14C11.6, destroy-

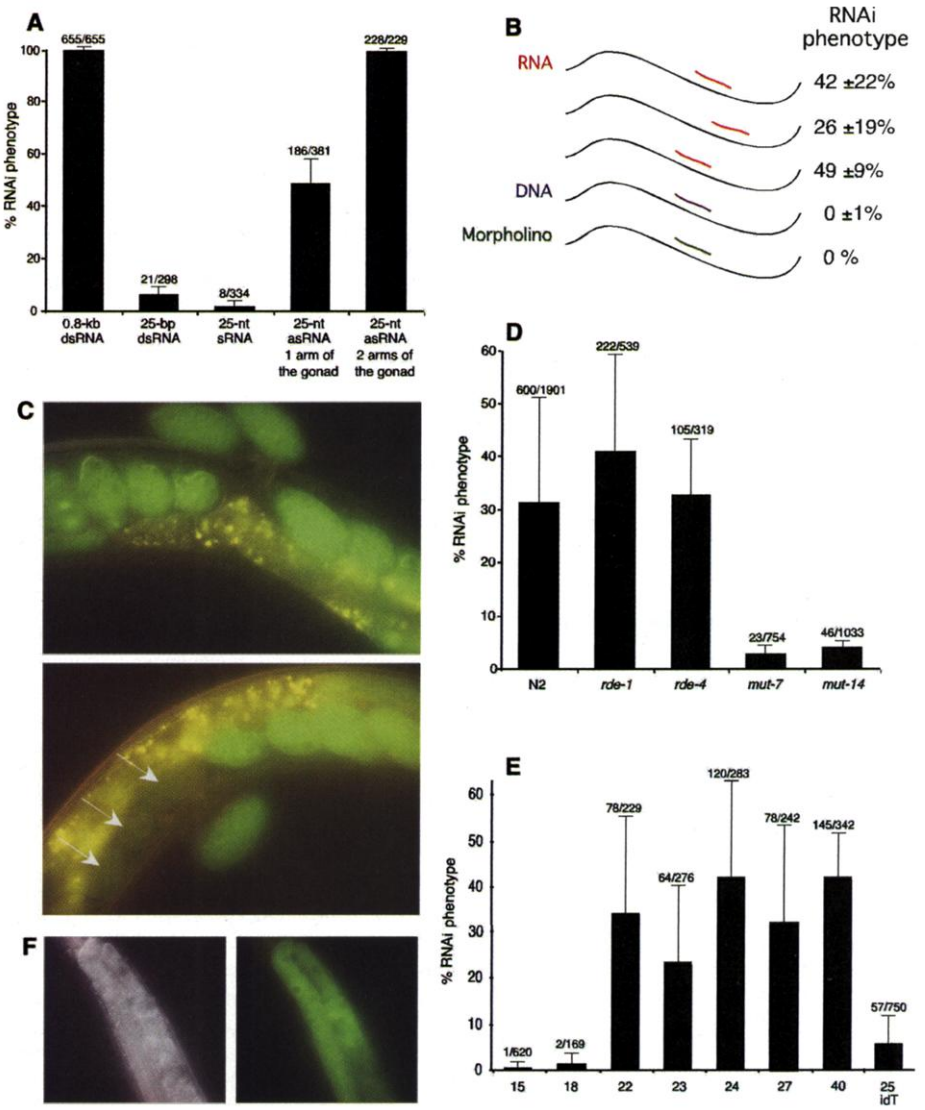

Fig. 1. asRNAs trigger gene silencing in *C. elegans*. **(A)** Different *pos-1* substrate RNAs were injected into one of two gonadal arms of the canonical *C. elegans* strain Bristol N2; the numbers of dead versus total embryos are indicated above the bars representing the percentage of the progeny that display the RNAi phenotype. Error bars reflect SD. **(B)** Interference activity of different types of nucleic acids. The top three lines reflect asRNAs directed against nonoverlapping *pos-1* sequences. **(C)** Animals that express GFP in the germ line and early embryos were injected with GFP asRNAs. Both panels show the midbody, with embryos on both sites of the vulva. Noninjected animals (upper panel) display a symmetrical pattern of GFP-expressing embryos coming from both oppositely located gonadal arms. Injected animals (bottom panel) display a reduced level of GFP expression in the embryos (white arrows) coming from the injected gonadal arm. **(D)** RNAi-deficient strains *rde-1*, *rde-4*, *mut-7*, and *mut-14* were assayed with 25-nt *pos-1* asRNAs. One gonadal arm was injected. **(E)** *pos-1* asRNAs of the indicated length were assayed for inducing gene silencing. idT marks asRNAs containing a 3′-inverted deoxythymidine. **(F)** Posterior gonad of *dcr-1* animals assayed as described in (C).

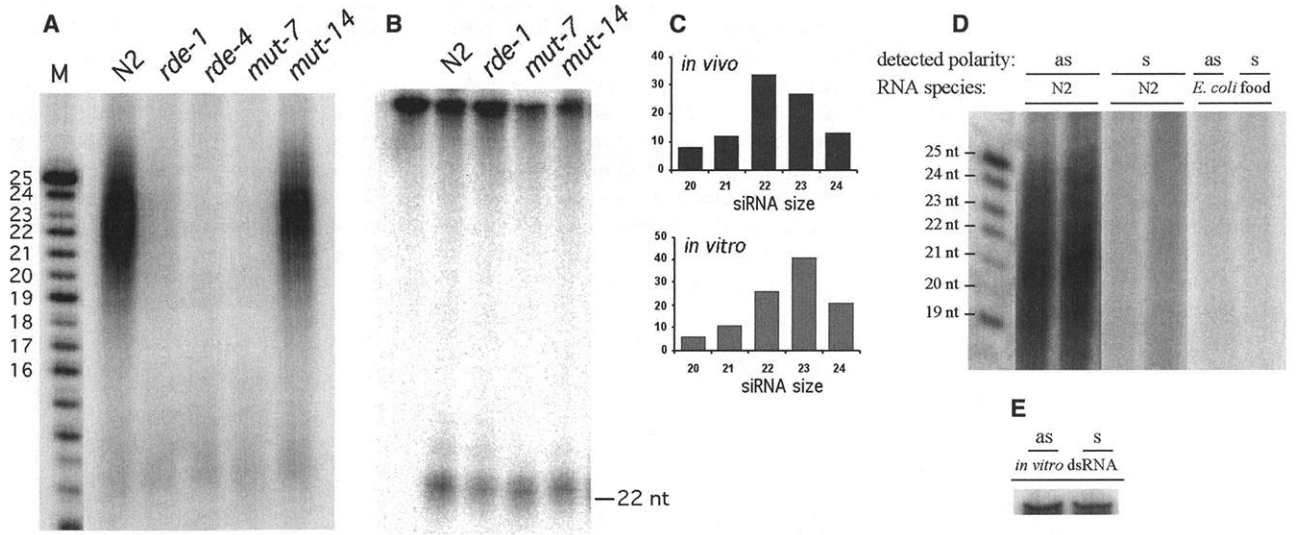

Fig. 2. siRNAs in *C. elegans* RNAi. **(A)** RNase protection assay on RNA isolated from wild-type (N2) and *rde-1*, *rde-4*, *mut-7*, and *mut-14* animals that were exposed to dsRNA (*11*). M indicates RNA size markers. **(B)** siRNA production in *C. elegans* extract: long dsRNA incubated with extracts prepared from wild-type (N2), *rde-1*, *mut-7*, and *mut-14* animals. **(C)** Size distribution of siRNAs produced in vivo and in vitro. **(D)** siRNA detection, in duplicate, in *pos-1* dsRNA-exposed N2 animals, with *pos-1* strand-specific probes. The detected polarity is indicated: sense (s) and antisense (as). As a control, the source of the dsRNA (*Escherichia coli* clones that produce *pos-1* dsRNA) was assayed. **(E)** Ribonuclease T1–treated, in vitro–prepared dsRNA was assayed to control for hybridization efficiencies.

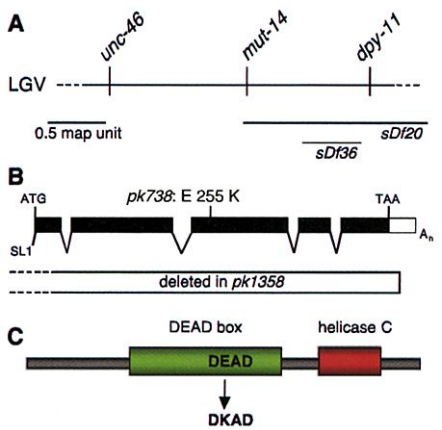

Fig. 3. Molecular identification of *mut-14*. **(A)** The location of *mut-14* on the *C. elegans* genetic map. **(B)** Structure of the C14C11.6 gene. The trans-spliced leader SL1, the initiation and stop codons, the poly(A) tail, and the position of the mutations in *pk738* and *pk1358* are indicated. **(C)** Domain structure of C11C14.6 showing the amino acid change of glutamic acid (E) into a lysine (K) at position 255 in *pk738*.

ing a consensus DEAD box motif by changing the glutamic acid at position 255 into a lysine. We isolated a deletion allele, *pk1358*, in which the complete C14C11.6 open reading frame and approximately 1 kb of upstream sequences are absent. *pk1358* animals display an RNAi-deficient phenotype, and *pk1358* failed to complement *pk738*. A DNA fragment containing C14C11.6 rescued the RNAi-defective phenotype of *pk738* animals. Based on these findings, we conclude that *mut-14* is the C14C11.6 gene.

The MUT-14 protein belongs to the evolutionary conserved superfamily of putative RNA helicases. Members of this family that contain the signature DEAD box motif are involved in diverse cellular functions; pre-mRNA splicing; rRNA processing; and mRNA export, translation, and degradation (*14*). At present, several RNA helicases have been implicated in posttranscriptional gene regulation and in transposon silencing (*15–17*). These proteins are similar to but clearly not orthologs of MUT-14. We found that MUT-14, apart from being involved in RNAi, is essential for gene silencing triggered by asRNAs, thus placing the action of this protein downstream of these molecules.

So where do these asRNAs fit in the RNAi pathway? One possibility is that the first step of RNAi (that is, long dsRNA diced into siRNAs) is bypassed by the administration of antisense oligomers. This predicts that asRNAs will also bypass the requirement for DCR-1, the protein that fulfills this function in RNAi (*12*, *18–20*). However, we failed to observe silencing of germline-expressed GFP in *dcr-1* animals that were injected with GFP asRNAs (Fig. 1F). Furthermore, if the asRNAs were to function as siRNAs, they should be incorporated in a multicomponent nuclease, designated RISC (*3*), that degrades homologous mRNAs. Recently, using a *Drosophila* cell-free system, it was found that synthetic ds-siRNAs lead to RISC (*21*) but only if they are of the right size: 20 to 23 nt but not longer (*4*, *22*). We found that 15- and 18-nt asRNAs were ineffective; but asRNAs of 22 nt and longer, up to 40 nt, were fully active to trigger gene silencing in *C. elegans* (Fig. 1E), suggesting that these asRNA molecules are taking another route to silence gene expression.

An alternative explanation is that asRNAs prime RNA synthesis on the mRNA, thus resulting in dsRNA that might then be a substrate for DICER-dependent degradation. This would explain why a broad range of asRNAs (22 to 40 nt long) is proficient in triggering gene silencing and why efficient gene silencing depends on the temporal coexistence of substrate and target. In favor of this idea, we observed that modifying the 3′ end of the asRNAs to prohibit polymerase action reduces the efficiency of gene silencing severely (Fig. 1E). The helicase activity of MUT-14 might thus act to permit de novo RNA synthesis on the target. Indeed, putative RNA-dependent RNA polymerases (RdRPs) are involved in RNAi and posttranscriptional gene silencing (PTGS) (*23–26*). In addition, biochemical and genetic support for RdRP action in amplifying the RNAi response was recently obtained (*11*, *27*). In *C. elegans*, *ego-1* is required for RNAi of germ line–expressed genes (*23*); unfortunately, we could not address the role of EGO-1 directly because of sterility and strongly disrupted gonads in *ego-1* mutants.

In striking similarity to the phenomenon of co-suppression, silencing induced by asRNAs requires the action of mutator/RNAi genes such as *mut-7* and *mut-14* but is independent of the RNAi-only genes *rde-1* and *rde-4*. This was also observed in RNAi for an "inherited interfering agent" that was inferred from genetic analysis (*28*). It has previously

been suggested for PTGS that "aberrant RNAs" produced by transgenes are triggering co-suppression (*18*, *29*). Possibly, these short asRNAs mimic such aberrant RNAs.

References and Notes

1. A. J. Hamilton, D. C. Baulcombe, *Science* **286**, 950 (1999).
2. P. D. Zamore, T. Tuschl, P. A. Sharp, D. P. Bartel, *Cell* **101**, 25 (2000).
3. S. M. Hammond, E. Bernstein, D. Beach, G. J. Hannon, *Nature* **404**, 293 (2000).
4. S. M. Elbashir, W. Lendeckel, T. Tuschl, *Genes. Dev.* **15**, 188 (2001).
5. S. Parrish, J. Fleenor, S. Xu, C. C. Mello, A. Fire, *Mol. Cell* **6**, 1077 (2000).
6. H. Tabara *et al.*, *Cell* **99**, 123 (1999).
7. R. F. Ketting, T. H. Haverkamp, H. G. van Luenen, R. H. Plasterk, *Cell* **99**, 133 (1999).
8. RNA oligonucleotides, obtained from Dharmacon Research (LaFayette, CO), contained a 5′ phosphate group; sequences are available on request. The asRNAs were injected at a concentration of 100 μM in water. dsRNA oligos were injected in 25 mM NaCl and 0.8 kb of *pos-1* dsRNA was injected at 200 ng/μl. The progeny of injected animals, collected in a 24-hour time frame (starting 16 hours after injection), were scored. Strain AZ244, which contains a *pie-1* promoter–driven GFP-tubulin protein fusion, was used to target germline-expressed GFP. Mutant alleles that were used are *rde-1(ne219)*, *rde-4(ne299)*, *mut-7(pk204)*, *mut-14(pk738)*, and *dcr-1* (*pk1351*).
9. M. Tijsterman, R. F. Ketting, K. L. Okihara, T. Sijen, R. H. A. Plasterk, data not shown.
10. R. F. Ketting, R. H. Plasterk, *Nature* **404**, 296 (2000).
11. T. Sijen *et al.*, *Cell* **107**, 1 (2001).
12. R. F. Ketting *et al.*, *Genes. Dev.* **15**, 2654 (2001).
13. *mut-14(pk738)* was isolated in a genetic screen (*7*) for germline transposon activation. Standard genetic techniques were used to map *mut-14* (*pk738*). A deletion allele, *mut-14(pk1358)*, which deletes nt 16252 through 18924 of C14C11, was isolated from a deletion library. Polymerase chain reaction–generated DNA fragments (5 ng/μl) spanning the C14C11.6 locus (nt 15241 through 19170 of C14C11) were co-injected with marker pRF4 (100 ng/μl) into *mut-14(pk738)* animals. Transgenic lines were scored for RNAi sensitivity.
14. J. de la Cruz, D. Kressler, P. Linder, *Trends. Biochem. Sci.* **24**, 192 (1999).
15. M. E. Domeier *et al.*, *Science* **289**, 1928 (2000).
16. T. Dalmay, R. Horsefield, T. Hartig Braunstein, D. C. Baulcombe, *EMBO J.* **20**, 2069 (2001).
17. D. Wu-Scharf, B. Jeong, C. Zhang, H. Cerutti, *Science* **290**, 1159 (2000).
18. E. Bernstein A. A. Caudy, S. M. Hammond, G. J. Hannon, *Nature* **409**, 363 (2001).
19. A. Grishok *et al.*, *Cell* **106**, 23 (2001).
20. S. W. Knight, B. L. Bass, *Science* **293**, 2269 (2001).
21. A. Nykanen, B. Haley, P. D. Zamore, *Cell* **107**, 309 (2001).
22. S. M. Elbashir, J. Martinez, A. Patkaniowska, W. Lendeckel, T. Tuschl, *EMBO J.*, in press.
23. A. Smardon *et al.*, *Curr. Biol.* **10**, 169 (2000).
24. C. Cogoni, G. Macino, *Nature* **399**, 166 (1999).
25. T. Dalmay, A. Hamilton, S. Rudd, S. Angell, D. C. Baulcombe, *Cell* **101**, 543 (2000).
26. P. Mourrain *et al.*, *Cell* **101**, 533 (2000).
27. C. Lipardi, Q. Wei, B. P. Paterson, *Cell* **107**, 297 (2001).
28. A. Grishok, H. Tabarah, C. C. Mello, *Science* **287**, 2494 (2000).
29. D. C. Baulcombe, *Science* **290**, 1108 (2000)

30. We thank J. Ahringer, A. Fire, H. Tabara, C. Mello, and A. Coulson for reagents; the Caenorhabditis Genetic Stock Center for strains; and M. van der Horst, K. Thijssen, and E. Cuppen for generating the knockout library.

29 October 2001; accepted 10 December 2001